PHILOSOPHICAL TRANSACTIONS A

rsta.royalsocietypublishing.org

Research

Cite this article: Galenko PK, Nizovtseva IG, Reuther K, Rettenmayr M. 2018 Kinetic transition in the order–disorder transformation at a solid/liquid interface. *Phil. Trans. R. Soc. A* **376**: 20170207.
http://dx.doi.org/10.1098/rsta.2017.0207

Accepted: 4 September 2017

One contribution of 16 to a theme issue 'From atomistic interfaces to dendritic patterns'.

Subject Areas:
materials science, solid state physics, mathematical modelling

Keywords:
long-range order parameter, kinetic phase transition, diffuse interface, ordering crystal, disorder trapping

Author for correspondence:
M. Rettenmayr
e-mail: M.Rettenmayr@uni-jena.de

Kinetic transition in the order–disorder transformation at a solid/liquid interface

P. K. Galenko[1], I. G. Nizovtseva[1,2], K. Reuther[1] and M. Rettenmayr[1]

[1]Otto-Schott-Institut für Materialforschung, Physikalisch-Astronomische Fakultät, Friedrich-Schiller-Universität Jena, 07743 Jena, Germany
[2]Department of Theoretical and Mathematical Physics, Laboratory of Multi-Scale Mathematical Modelling, Ural Federal University, Ekaterinburg 620000, Russian Federation

PKG, 0000-0003-2941-7742; MR, 0000-0003-4721-5087

Phase-field analysis for the kinetic transition in an ordered crystal structure growing from an undercooled liquid is carried out. The results are interpreted on the basis of analytical and numerical solutions of equations describing the dynamics of the phase field, the long-range order parameter as well as the atomic diffusion within the crystal/liquid interface and in the bulk crystal. As an example, the growth of a binary $A_{50}B_{50}$ crystal is described, and critical undercoolings at characteristic changes of growth velocity and the long-range order parameter are defined. For rapidly growing crystals, analogies and qualitative differences are found in comparison with known non-equilibrium effects, particularly solute trapping and disorder trapping. The results and model predictions are compared qualitatively with results of the theory of kinetic phase transitions (Chernov 1968 *Sov. Phys. JETP* **26**, 1182–1190) and with experimental data obtained for rapid dendritic solidification of congruently melting alloy with order–disorder transition (Hartmann *et al.* 2009 *Europhys. Lett.* **87**, 40007 (doi:10.1209/0295-5075/87/40007)).

This article is part of the theme issue 'From atomistic interfaces to dendritic patterns'.

THE ROYAL SOCIETY PUBLISHING

1. Introduction

The transition from a long-range-ordered to a disordered crystal structure is a phenomenon which is observed in congruently melting alloys that solidify with high crystal growth velocities [1]. Such transitions have been studied both experimentally by characterizing growth conditions and microstructures of congruently melting alloys [2–5], and theoretically by continuum [6–8] and discrete atomistic models [9,10]. In these studies, the formation of a disordered crystal is interpreted as disorder trapping of the atoms in the liquid by the rapidly moving interface [6]. This is analogous to the trapping of defects [11] or solute atoms by rapid interfaces [11–15]. Physically, disorder trapping implies that the crystal/liquid interface moves so fast that the period of time that is needed for short-range diffusion to establish a long-range-ordered crystal is not available. Experimental evidence of disorder trapping has been found by *in situ* diffraction studies using synchrotron radiation on levitation-processed samples, in which a transition from ordered to disordered growth at a critical undercooling was shown [3].

Chernov was the first who explained the sharp change of the long-range order parameter in the structure of a rapidly growing crystal [16,17]. He showed that with increasing deviation from equilibrium, the long-range order parameter sharply decreases down to zero, at which point the crystal growth velocity increases sharply. Chernov called this behaviour a kinetic phase transition in which supersaturation plays the role of temperature as generally known in general (thermodynamic) phase transitions. One of the main features of the kinetic phase transition is that it occurs due to the finite speed of atomic diffusion on the sites of the crystal lattice [18].

On the basis of his kinetic model of cooperative atomistic phenomena, Chernov stated that the kinetic phase transition can be regarded analogously to a thermodynamic phase transition of second order with increasing deviation from local thermodynamic equilibrium (i.e. increasing supersaturation or undercooling). Possibly, the analogy can be extended to a first-order phase transition from a metastable to a stable crystal. This conclusion was derived from the model which considers the ordering directly at the crystal/liquid interface [16]. Following Chernov's work, Brener & Temkin [19,20] provided an extended analysis of the ordering kinetics occurring both at the crystal/liquid interface and in an ordering zone behind the interface in the bulk crystal. They assumed that crystallization proceeds without change of chemical composition and that the ordering itself can be considered as a transition of the first or second order. The solution to their equations yielded both the crystal growth velocity and the distribution of the long-range order parameter as functions of temperature. In all considered cases, the theories [19,20] predicted the existence of a critical point for the transition from ordered growth to disordered growth in which the crystal velocity may have either an abrupt or a smooth rise.

Brener & Temkin [19,20] analysed ordering in the close vicinity of the point of kinetic phase transition where the ordering zone is much wider than the diffuse interface between crystal and liquid. Therefore, they used the Ginzburg–Landau functional and time-dependent relaxation equation for the diffuse zone of the long-range order parameter and atomic kinetics at the sharp crystal/liquid interface. Extending the analysis, the present work shows results describing the order–disorder transition in a wide range of crystal growth velocities and with two competing diffuse regions, namely the crystal/liquid interface and the ordering zone. The results are obtained using the phase-field theory [21,22], which allows us to analyse the simultaneous relaxation of two or more order parameters with different characteristic widths [23]. To investigate both slow growth under near-equilibrium conditions with complete ordering and rapid growth far from equilibrium with complete disordering, a model of fast phase transformations [24] is applied to the 'liquid–crystal' transition with ordering. In the numerical solutions of the model, we show the existence of pronounced disorder trapping by a direct exchange of dissimilar atoms between sublattices at interfaces moving with high velocities into an undercooled binary liquid. The main focus of the present work is to formulate conditions for disorder trapping in undercooled, rapidly transforming congruently melting alloys in the liquid state. We show that the absence of a direct exchange of dissimilar atoms between sublattices, which is a consequence of a rapidly moving crystal/liquid interface, leads to partial or complete disorder trapping.

2. Conditions for the order–disorder transformation in a growing crystal

Depending on the velocities of (i) the diffuse interface during the liquid–crystal transformation and (ii) the ordering zone, one can formulate conditions for disorder trapping and for the formation of an ordered or disordered structure of a crystal. Disorder trapping occurs when an atom that attaches to the crystal has no time to find its thermodynamic equilibrium position. The atom is trapped by the diffuse interface and remains at an energetically less favourable non-equilibrium position. This occurs if the velocity of the diffuse crystal/liquid interface V is faster than the ordering velocity $V_{DT} \propto D_\eta/\delta_\eta$, where $D_\eta = M_\eta \varepsilon_\eta$ is the diffusion coefficient, M_η is the atomic mobility and ε_η is the gradient factor showing the strength of the long-range order variation, which can be considered as the driving force for the ordering process. These kinetic coefficients define the period of time for an atom to find an energetically favourable position in the crystal that forms in the ordering zone with width δ_η. If $V > V_{DT}$, the time δ_φ/V for the transformation within the width δ_φ of the diffuse crystal/liquid interface becomes smaller than the time δ_η^2/D_η that is necessary for complete ordering in the lattice. Thus, disorder trapping proceeds under the following kinetic conditions:

$$\left.\begin{aligned} & V > \frac{D_\eta}{\delta_\eta} \\ \text{and} \quad & t_\delta = \frac{\delta_\varphi}{V} < t_\eta = \frac{\delta_\eta^2}{D_\eta} = \frac{\delta_\eta}{V_{DT}}. \end{aligned}\right\} \tag{2.1}$$

From these conditions it follows that the critical velocity for disorder trapping V_{DT} decreases with increase in the ratio $\delta_\eta/\delta_\varphi$. As a result, one gets

$$\left.\begin{aligned} & \text{critical velocity for the beginning of disorder trapping:} \quad V_{DT} = \frac{\delta_\eta}{\delta_\varphi} V, \\ & \text{formation of an ordered crystal if} \quad V < V_{DT} \\ \text{and} \quad & \text{formation of a disordered crystal if} \quad V > V_{DT}. \end{aligned}\right\} \tag{2.2}$$

From the inequalities of equation (2.2), two obvious conditions follow: (i) disorder trapping increases with increasing velocity V and decreasing diffuse interface width δ_φ; (ii) for shrinking width of the ordering zone, the critical velocity for disorder trapping increases.

These conditions for disorder trapping are demonstrated in figure 1. Complete ordering under the conditions for the formation of a crystal superlattice with $\delta_\eta < \delta_\varphi$ is illustrated in figure 1*a*. The beginning of disorder trapping occurs if $\delta_\eta > \delta_\varphi$; figure 1*b*. Pronounced disorder trapping is found with $\delta_\eta \gg \delta_\varphi$; figure 1*c*. Finally, complete disorder trapping occurs if $\delta_\eta \to \infty$, as shown in figure 1*d*. From these conditions it follows that the assumption of a sharp crystal/liquid interface [19,20] can only describe the last two cases, i.e. the ones shown in figure 1*c*,*d*. The diffuse interface in this work describes the complete scenario of figure 1*a*–*d*.

3. Definitions

(a) Main functions

We consider a binary mixture consisting of A atoms and B atoms. At a given temperature T, the main functions of the model, for which solutions are sought, are defined as follows. The *first function* is the phase field φ with $\varphi = 1$ in the crystal and $\varphi = 0$ in the liquid. The *second function* is the overall continuous concentration of B atoms x_B (which can be defined through the compositions of the crystal and the liquid). Concentrations in the crystal are given by $x_i^j = n_i^j/(n_A^j + n_B^j)$, where n_i^j is the number of moles of atoms i ($i = A, B$) on the sublattice j ($j = \alpha, \beta$).

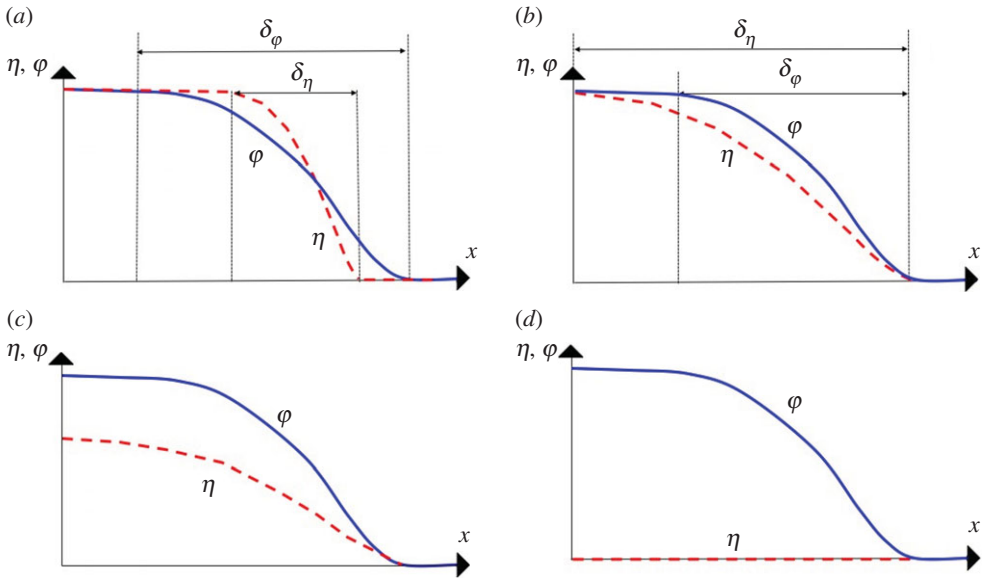

Figure 1. Position of the phase-field φ profile relative to the profile of the long-range order parameter η. (*a*) Complete ordering during sluggish crystal growth. The ordering zone is smaller than the width of the diffuse crystal/liquid interface, $\delta_\eta < \delta_\varphi$. (*b*) Beginning of disorder zone formation, $\delta_\eta > \delta_\varphi$. (*c*) Pronounced disorder in the crystal at high velocity of the crystal/liquid interface, $\delta_\eta \gg \delta_\varphi$. (*d*) Complete disorder under rapid solidification conditions, $\delta_\eta \to \infty$.

The *third function* is the long-range order parameter η, which is defined by the concentrations $y_i^j = (y_A^\alpha, y_A^\beta, y_B^\alpha, y_B^\beta)$ of the α and β sublattices as

$$\eta = y_A^\alpha - y_A^\beta = y_B^\beta - y_B^\alpha. \tag{3.1}$$

A completely disordered state in the crystal is described by $\eta = 0$. The state is fully ordered on the sublattices when $\eta = 1$. The concentrations in the crystal on the sublattices are

$$y_A^\alpha = 1 - \left(x_B - \frac{\eta}{2}\right), \quad y_B^\alpha = x_B - \frac{\eta}{2} \tag{3.2}$$

and

$$y_A^\beta = 1 - \left(y_B + \frac{\eta}{2}\right), \quad y_B^\beta = x_B + \frac{\eta}{2}. \tag{3.3}$$

(b) Gibbs free energy

(i) The entire system

The Gibbs free energy for the entire binary system is given by

$$G(\varphi, \nabla\varphi, \eta, \nabla\eta, x_B) = G_S(x_B, \eta)p(\varphi) + G_L(x_B)[1 - p(\varphi)] + \frac{\varepsilon_\varphi}{2}(\nabla\varphi)^2 + \frac{\varepsilon_\eta}{2}(\nabla\eta)^2 + W_\varphi g_\varphi(\varphi) + W_\eta g_\eta(\eta). \tag{3.4}$$

The double-well functions in equation (3.4) for the phase field g_φ and for the long-range order parameter g_η are given by

$$g_\varphi(\varphi) = \varphi^2(1-\varphi)^2 \quad \text{and} \quad g_\eta(\eta) = \eta^2(1-\eta)^2. \tag{3.5}$$

The Gibbs free energy is interpolated between the phases using the following function:

$$p(\varphi) = \varphi^2(3 - 2\varphi). \tag{3.6}$$

(ii) The phases

In the liquid phase, we assume the following approximation:

$$G_{\mathrm{L}}(T,x_{\mathrm{B}}) = (1-x_{\mathrm{B}})G_{\mathrm{L}}^{\mathrm{A}}(T) + x_{\mathrm{B}}G_{\mathrm{L}}^{\mathrm{B}}(T), \tag{3.7}$$

$$G_{\mathrm{L}}^{\mathrm{A}}(T,x_{\mathrm{B}}) = G_{\mathrm{L}}^{0\mathrm{A}}(T) + RT\ln(1-x_{\mathrm{B}}) + x_{\mathrm{B}}\Omega_{\mathrm{L}} \tag{3.8}$$

and

$$G_{\mathrm{L}}^{\mathrm{B}}(T,x_{\mathrm{B}}) = G_{\mathrm{L}}^{0\mathrm{B}}(T) + RT\ln(x_{\mathrm{B}}) + (1-x_{\mathrm{B}})\Omega_{\mathrm{L}}. \tag{3.9}$$

This can be regarded as contributions from the elements A and B (3.7), reference terms G_{L}^{0i}, ideal mixture terms $RT\ln x_i$ and excess terms $x_i\Omega_{\mathrm{L}}$ (where again $i=\mathrm{A},\mathrm{B}$).

In the crystal, the Gibbs free energy has additional terms related to the disorder parameter:

$$G_{\mathrm{S}}(T,x_{\mathrm{B}},\eta) = G_{\mathrm{S}}^{\mathrm{ref}}(T,x_{\mathrm{B}}) + G_{\mathrm{S}}^{\mathrm{id}}(T,x_{\mathrm{B}},\eta) + G_{\mathrm{S}}^{\mathrm{ex}}(x_{\mathrm{B}},\eta). \tag{3.10}$$

Assuming that the liquid transforms into the body-centred cubic (bcc) structure, the following contributions to the Gibbs free energy (3.10) are taken into account: the reference contribution

$$G_{\mathrm{S}}^{\mathrm{ref}}(T,x_{\mathrm{B}}) = (1-x_{\mathrm{B}})G_{\mathrm{A}}^{\mathrm{bcc}}(T) + x_{\mathrm{B}}G_{\mathrm{B}}^{\mathrm{bcc}}(T), \tag{3.11}$$

the ideal mixture contribution

$$\begin{aligned} G_{\mathrm{S}}^{\mathrm{id}}(T,x_{\mathrm{B}},\eta) = \frac{RT}{2}\Big[&\Big(x_{\mathrm{B}}-\frac{\eta}{2}\Big)\ln\Big(x_{\mathrm{B}}-\frac{\eta}{2}\Big) + \Big(x_{\mathrm{B}}+\frac{\eta}{2}\Big)\ln\Big(x_{\mathrm{B}}+\frac{\eta}{2}\Big) \\ &+ \Big(1-x_{\mathrm{B}}-\frac{\eta}{2}\Big)\ln\Big(1-x_{\mathrm{B}}-\frac{\eta}{2}\Big) + \Big(1-x_{\mathrm{B}}+\frac{\eta}{2}\Big)\ln\Big(1-x_{\mathrm{B}}+\frac{\eta}{2}\Big)\Big] \end{aligned} \tag{3.12}$$

and the excess free energy

$$G_{\mathrm{S}}^{\mathrm{ex}}(x_{\mathrm{B}},\eta) = \Omega_2\left(x_{\mathrm{B}}(1-x_{\mathrm{B}}) + \frac{\eta^2}{4}\right) + \Omega_3\eta^3 + \Omega_4\eta^4. \tag{3.13}$$

4. Governing equations

Following the model of fast phase transformations [24], one can derive the governing hyperbolic equations for non-conserved and conserved field variables. They are obtained by the condition of non-decreasing entropy in time, which, for isothermal systems, is equivalent to the condition of non-increasing Helmholtz free energy in time [25]. Following these approaches [24,25], one can derive the system of governing equations using the Gibbs free energies from §3b as thermodynamic potentials accessible from thermodynamic databases. Then, one can find the governing equations for: the phase field

$$\tau_\varphi\frac{\partial^2\varphi}{\partial t^2} + \frac{\partial\varphi}{\partial t} = -M_\varphi\frac{\delta G}{\delta\varphi}, \tag{4.1}$$

the long-range order parameter

$$\tau_\eta\frac{\partial^2\eta}{\partial t^2} + \frac{\partial\eta}{\partial t} = -M_\eta\frac{\delta G}{\delta\eta} \tag{4.2}$$

and the concentration and chemical potential

$$\tau_D\frac{\partial^2 x_{\mathrm{B}}}{\partial t^2} + \frac{\partial x_{\mathrm{B}}}{\partial t} = \nabla\cdot(M_x\nabla\mu_{\mathrm{B}}), \quad \mu_{\mathrm{B}} = \frac{\delta G}{\delta x_{\mathrm{B}}}. \tag{4.3}$$

The hyperbolic equations (4.1) and (4.2) are damped wave equations, which extend the known parabolic equation for non-conserved order parameters derived first by Mandel'shtam & Leontovich [26,27] and called in the literature the time-dependent Ginzburg–Landau equation [27,28] and the Allen–Cahn equation [29]. The hyperbolic equation (4.3) generalizes the known parabolic equation for conserved order parameters. Equations (4.1)–(4.3) have been successfully applied to non-monotonic relaxation [30] and phase segregation [31]. They were analysed in the context of fast dynamics during transitions from unstable to metastable or metastable to stable

states [32]. The validity of hyperbolic models in fast phase transition theory has been verified by comparison with experimental data [33] in molecular dynamics simulations of solute trapping by rapidly moving interfaces [34] and by coarse-graining derivations of phase-field equations [35].

(a) Phase field

In its explicit form, the governing equation for the phase field is deduced from equations (3.4)–(4.1). As a result, one finds

$$\begin{aligned}\frac{\tau_\varphi}{M_\varphi}\frac{\partial^2\varphi}{\partial t^2}+\frac{1}{M_\varphi}\frac{\partial\varphi}{\partial t}&=\varepsilon_\varphi\nabla^2\varphi-W_\varphi\frac{\mathrm{d}g_\varphi(\varphi)}{\mathrm{d}\varphi}\\&-\Bigg[(1-x_\mathrm{B})G_\mathrm{B}^\mathrm{bcc}+x_\mathrm{B}G_\mathrm{B}^\mathrm{bcc}+\frac{RT}{2}\Bigg(\Bigg(\frac{x_\mathrm{B}-\eta}{2}\Bigg)\ln\Big(x_\mathrm{B}-\frac{\eta}{2}\Big)+\Big(x_\mathrm{B}+\frac{\eta}{2}\Big)\ln\Big(x_\mathrm{B}+\frac{\eta}{2}\Big)\\&+\Big(1-x_\mathrm{B}-\frac{\eta}{2}\Big)\ln\Big(1-x_\mathrm{B}-\frac{\eta}{2}\Big)+\Big(1-x_\mathrm{B}+\frac{\eta}{2}\Big)\ln\Big(1-x_\mathrm{B}+\frac{\eta}{2}\Big)\Bigg)\\&+\Omega_2\Big(x_\mathrm{B}(1-x_\mathrm{B})+\frac{1}{4}\eta^2\Big)+\Omega_3\eta^3+\Omega_4\eta^4\Bigg]\frac{\mathrm{d}p(\varphi)}{\mathrm{d}\varphi}\\&-[(1-x_\mathrm{B})(G_\mathrm{L}^{0\mathrm{A}}+RT\ln(1-x_\mathrm{B})+x_\mathrm{B}\Omega_\mathrm{L})+x_\mathrm{B}(G_\mathrm{L}^{0\mathrm{B}}+RT\ln(x_\mathrm{B})+(1-x_\mathrm{B})\Omega_\mathrm{L})]\frac{\mathrm{d}p(\varphi)}{\mathrm{d}\varphi}.\end{aligned}\tag{4.4}$$

Without the ordering process, i.e. if $\eta=0$, equation (4.4) transforms into the equation derived in [24,25].

(b) Order parameter

Atomic ordering in the α and β sublattices is described by equation (4.2) together with the Gibbs free energy (3.4)–(3.13) as

$$\begin{aligned}\frac{\tau_\eta}{M_\eta}\frac{\partial^2\eta}{\partial t^2}+\frac{1}{M_\eta}\frac{\partial\eta}{\partial t}&=\varepsilon_\eta\nabla^2\eta-W_\eta\frac{\mathrm{d}g_\eta(\eta)}{\mathrm{d}\eta}-\Bigg[\frac{RT}{2}\Bigg(-\frac{1}{2}\ln\Big(x_\mathrm{B}-\frac{\eta}{2}\Big)+\frac{1}{2}\ln\Big(x_\mathrm{B}+\frac{\eta}{2}\Big)\\&-\frac{1}{2}\ln\Big(1-x_\mathrm{B}-\frac{\eta}{2}\Big)+\frac{1}{2}\ln\Big(1-x_\mathrm{B}+\frac{\eta}{2}\Big)\Bigg)+\frac{1}{2}\Omega_2\eta+3\Omega_3\eta^2+4\Omega_4\eta^3\Bigg]p(\varphi).\end{aligned}\tag{4.5}$$

From equation (4.5) it follows that the process of atomic ordering is coupled to the phase field by the interpolation function $p(\varphi)$.

(c) Chemical diffusion

The chemical potential from equation (4.3) is given by the variational derivative

$$\begin{aligned}\mu_\mathrm{B}=\frac{\delta G}{\delta x_\mathrm{B}}&=\Bigg[G_\mathrm{B}^\mathrm{bcc}-G_\mathrm{B}^\mathrm{bcc}+\frac{\mathrm{RT}}{2}\Big(\ln\Big(x_\mathrm{B}-\frac{\eta}{2}\Big)+\ln\Big(x_\mathrm{B}+\frac{\eta}{2}\Big)-\ln\Big(1-x_\mathrm{B}-\frac{\eta}{2}\Big)\\&-\ln\Big(1-x_\mathrm{B}+\frac{\eta}{2}\Big)\Big)+\Omega_2(1-2x_\mathrm{B})\Bigg]p(\varphi)+[G_\mathrm{L}^{0\mathrm{B}}-G_\mathrm{L}^{0\mathrm{A}}+RT(\ln(x_\mathrm{B})-\ln(1-x_\mathrm{B}))\\&+2(1-2x_\mathrm{B})\Omega_\mathrm{L}]p(1-\varphi).\end{aligned}\tag{4.6}$$

The mobility M_x in the diffusion equation (4.3) is an interpolation between the bulk mobilities in the liquid M_L and in the solid M_S:

$$\begin{aligned}M_x&=M_\mathrm{L}(1-p(\varphi))+M_\mathrm{S}(\eta)p(\varphi)\\&=M_\mathrm{L}(1-p(\varphi))+(M_\mathrm{S}^\mathrm{disorder}(1-\eta)+M_\mathrm{S}^\mathrm{order}\eta)p(\varphi).\end{aligned}\tag{4.7}$$

As follows from equation (4.7), the bulk mobility $M_\mathrm{S}(\eta)$ in the solid is interpolated by the atomic mobilities $M_\mathrm{S}^\mathrm{order}$ and $M_\mathrm{S}^\mathrm{disorder}$ in the ordered state and disordered state, respectively.

Table 1. Physical parameters of the $A_{50}B_{50}$ alloy used for modelling.

parameter	value and dimension
mole fraction of A(B), x_B	0.5
η-rate relaxation time, τ_η	4×10^{-8} s
φ-rate relaxation time, τ_φ	4×10^{-11} s
x_B-rate relaxation time, τ_D	4×10^{-10} s
mobility of the η field, M_η	8×10^{4} mol J^{-1} s^{-1}
mobility of the φ field, M_φ	4×10^{5} mol J^{-1} s^{-1}
mobility of B atoms in the l phase, M_L	2×10^{-8} mol m^2 J^{-1} s^{-1}
mobility of B atoms in the disordered state, $M_S^{disorder}$	7×10^{-11} mol m^2 J^{-1} s^{-1}
mobility of B atoms in the ordered state, M_S^{order}	9×10^{-12} mol m^2 J^{-1} s^{-1}
gradient factor for the η field, ε_η	1.4×10^{-13} J m^2 mol^{-1}
gradient factor for the φ field, ε_φ	5.5×10^{-12} J m^2 mol^{-1}
energy barrier between states in the η field, W_η	2.5×10^{3} J mol^{-1}
energy barrier between states in the φ phase, W_φ	4.5×10^{3} J mol^{-1}
1st thermodynamic parameter[a], Ω_2	$-2 \times 10^{3}R$ J mol^{-1}
2nd thermodynamic parameter, Ω_3	$-1.225 \times 10^{6}R$ J mol^{-1}
3rd thermodynamic parameter[a], Ω_4	$-5.662 \times 10^{2}R$ J mol^{-1}
4th thermodynamic parameter[a], Ω_L	-1.72×10^{4} J mol^{-1}

[a]Data are from [6]. All other parameters were chosen by the authors.

5. Material parameters and modelling

The spatially inhomogeneous evolution of ordered and disordered states is modelled by numerically solving the equations for diffusion (4.3), (4.6) and (4.7), phase-field motion (4.4) and ordering (4.5). Material parameters were chosen for a binary congruently melting $A_{50}B_{50}$ alloy (table 1). Functions $G_L^{0A}(T)$, $G_L^{0B}(T)$, $G_A^{bcc}(T)$ and $G_B^{bcc}(T)$ from equations (3.7)–(3.9) and (3.11) are taken from a thermodynamic database (CALPHAD) for a $Ni_{50}Al_{50}$ alloy. Because crystals in the $Ni_{50}Al_{50}$ alloy grow as for the congruently melting alloy, chemical segregation is absent. Therefore the system of diffusion equations (4.3), (4.6) and (4.7) has been written in the present work just for the completeness of the statement of the problem.

The numerical procedure for the solution of the model equations consists of a finite difference (FD) scheme of second order with explicit time stepping. The initial concentration distribution was taken to be homogeneous, $x_B = 0.5$, which implies a vanishing contribution of the chemical composition in the governing equations. The modelled situation therefore describes the growth of an ordered crystal without chemical segregation in the liquid, which is the case for congruently melting alloys. The phase field φ and order η parameters were initially set to unity in the solid and zero in the liquid, connected by a smooth transition at the interface, which was described by a Gaussian error function with a width of 1 µm, corresponding to 10 FD nodes. Boundary conditions were Dirichlet type on the solidifying side and Neumann type (zero flux) in the liquid far away from the interface.

Numerical solutions of equations (4.1)–(4.7) were achieved in a one-dimensional space. To obtain steady-state results, average values of the interface velocity V for the phase field and the long-range order parameter η were determined as follows: the phase field has a step-like shape with $\varphi = 1$ in the crystal and $\varphi = 0$ in the liquid. The crystal/liquid interface is a diffuse interface, and the conventional definition of the interface position is the point z_f where $\varphi(z_f) = 0.5$.

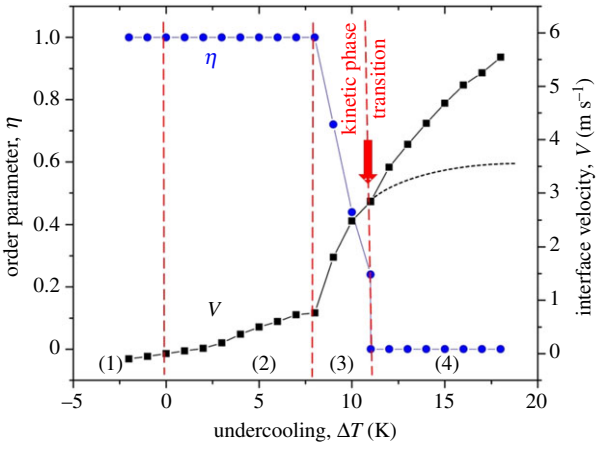

Figure 2. Crystal/liquid interface velocity V and long-range order parameter η as functions of undercooling in steady-state solidification, $\Delta T > 0$, and overheating in melting of a crystal, $\Delta T < 0$. Region (1) relates to 'melting'. Region (2) relates to 'sluggish growth of a completely ordered crystal'. Region (3) relates to 'growth of a disordered crystal'. Region (4) relates to 'growth with complete disorder trapping'. Shown by the arrow, the point of kinetic phase transition is consistent with the transition to complete disorder trapping and growth of a disordered crystal. The dotted line in region (4) shows the extrapolation of the growth velocity beyond the point of total solute trapping. In fact, at and behind the point of the kinetic transition, the rate of velocity change increases (solid line with squares in region (4)) due to the lack of energy dissipation at the formation of the superlattice.

In this work, we adopt another definition of the interface position, namely $z_f = \int_{-\infty}^{+\infty} \varphi(z')\,\mathrm{d}z'$. This definition is exact for the case of a symmetric interface profile and allows us to find an exact interface velocity in the case of an asymmetric steady-state profile. During the simulation run, we collect the values of the interface position z_f^n at time intervals t^n after a fixed number (e.g. 2000) of time steps. The interface velocity V is obtained as $V^n = (z_f^n - z_f^{n-1})/(t^n - t^{n-1})$. After the system reaches a steady-state regime, we calculate the *steady-state interface velocity* V^{avg} as the average of the last 10 values V^n. The *average value of the order parameter* η in the solid phase right behind the interface is determined as the average of 11 FD nodes at a distance of 10 FD spacings behind the interface, i.e. the FD nodes 10–20 behind the calculated interface position.

6. Kinetic transition

Figure 2 shows the dependence of the order parameter η and the interface velocity V on the undercooling ΔT for steady-state growth. Four different regions can be distinguished. Region (1) shows melting ($\Delta T < 0$ and $V < 0$) of the completely ordered crystal ($\eta = 1$) within the diffuse interface and in the bulk crystal. The point $\Delta T = 0$ shows the coexistence of the liquid and crystal phases. In region (2) the system exhibits ordered crystal growth with $V > 0$ and $\eta = 1$. Owing to the slow kinetics, the time for diffusion relaxation and for the formation of the long-range order is shorter than the solidification time. The superlattice of the crystal forms so fast that the width of the diffuse interface cannot oversweep the ordering zone δ_η (figure 1*a*).

With increasing undercooling and velocity, the transition from region (2) into region (3) occurs when the time for solidification becomes shorter than the time for ordering. The ordering zone becomes wider than the thickness of the diffuse interface, $\delta_\eta > \delta_\phi$, as shown in figure 1*b*. Region (3) can be characterized by the beginning of disorder trapping ($0 < \eta < 1$) together with a change of growth kinetics. In region (3), the velocity change of the diffuse interface responds more sensitively to the undercooling than in region (2). This is caused by the gradually decreasing energy required for the formation of the superlattice.

At the critical undercooling (indicated by an arrow in figure 2), the crystal growth velocity exhibits a sharp change in slope, and the long-range order parameter sharply decreases down to

zero.[1] This sharp drop in the order parameter at the critical undercooling leads to a discontinuity in the first derivative of the interface velocity that has been previously interpreted as a 'kinetic transition' [16–20]. In light of the present results, the kinetic transition shows a sharp change from partial disorder trapping in region (3) to complete disorder trapping in region (4) (which is schematically presented by figure 1*c*,*d*).

In conclusion, with increasing growth rate there are two transitions between ordered and completely disordered growth: (i) a transition from a completely ordered to a partially disordered structure (from region (2) to region (3)) and subsequently (ii) from a partially disordered structure to complete disorder (from region (3) to region (4)). Both transitions are accompanied by an increase in the sensitivity of the growth velocity to the undercooling, as the energy dissipated by the creation of the ordered lattice first decreases (in case (i)) and then completely vanishes (in case (ii)). This is demonstrated by the extrapolated $V-\Delta T$ curve in figure 2.

7. Further considerations

(a) Dendritic growth, disorder trapping and kinetic transition

Solute trapping and disorder trapping are well-known non-equilibrium effects which are observed at high growth velocities [2,4–8,13–15,34,36]. In the context of figure 2, the effect of the kinetic phase transition on microstructure formation during dendritic growth with disorder trapping can be evaluated.

Disorder trapping [6] occurs during rapid dendritic solidification of undercooled melts of intermetallics with superlattice structure [4,5,7]. In such systems, crystal growth is sluggish at small undercoolings [2]. Attachment of atoms from the liquid to the crystal requires short-range atomic diffusion, because atoms have to sort themselves to reach their proper position in the superlattice structure. With increasing undercooling, the non-equilibrium effect of disorder trapping leads to solidification of a metastable disordered structure [36]. This effect and the order–disorder transformation in dendrites have been investigated by Hartmann *et al.* [3] in experiments with droplets processed by electromagnetic levitation. These authors measured the dendrite growth velocity during solidification of the intermetallic compound $Ni_{50}Al_{50}$ undercooled in levitation up to 265 K. A sharp increase in the growth velocity with a change in slope of the relationship between crystal growth velocity V and undercooling ΔT was found by Hartmann *et al.* at a critical undercooling $\Delta T \approx 250$ K.

Ordered crystal growth from undercooled melts [3] exhibits an abrupt change in the $V-\Delta T$ curve at a critical value of the non-equilibrium parameter ΔT, which characterizes this phenomenon as a kinetic transition by the definition of Chernov [16]. Thus, the gathered experimental results and the theoretical predictions clearly demonstrate that the solidification of intermetallic phases out of undercooled melts exhibits a kinetic phase transition in the process of atomic ordering.

(b) Comparison with solute trapping

It is appropriate to compare the growth kinetics with the influence of solute trapping [12,13] and disorder trapping. Several analogies and one principal difference in these two phenomena can be outlined.

The first similarity is the fact that both solute trapping and disorder trapping lead to a metastable microstructure or crystal structure [9,14,33,37]. In this sense, Boettinger & Aziz [6] developed an early remarkable model for disorder trapping in which, during formation of the crystal lattice from a liquid, each sublattice captures atoms in a quantity that is not the equilibrium quantity.

[1]Owing to the use of a diffuse interface, the long-range order parameter η decreases to zero within a small interval of undercooling $\Delta T \approx 1$ K.

The second similarity can be found in the early stages of both phenomena. As shown experimentally by Eckler *et al.* [14], the beginning of solute trapping is characterized by a sudden increase in velocity. The same effect is observed at the beginning of disordered crystal formation (see the transition from region (2) into region (3) in figure 2).

A distinct difference can be found in the final stages of the two phenomena: complete solute trapping results in a decrease in growth velocity due to the abrupt vanishing of solutal undercooling in the total undercooling balance [38]. By contrast, the rate of change of growth velocity at and behind the point of complete disorder trapping increases due to the vanishing energy dissipation for the building of the superlattice. Despite this difference, however, the final stage of solute trapping can also be called a kinetic phase transition, because it is included in the definition of Chernov [6].

(c) Influence of local non-equilibrium effects

Equations (4.1)–(4.3) are partial differential equations of a hyperbolic type. Such equations describe the propagation of disturbances with finite velocities, in this case with: (i) the characteristic velocity of the η field $V_\eta = \sqrt{D_\eta/\tau_\eta}$, $D_\eta = M_\eta \varepsilon_\eta$; (ii) the characteristic velocity of the φ field $V_\varphi = \sqrt{D_\varphi/\tau_\varphi}$, $D_\varphi = M_\varphi \varepsilon_\varphi$; and (iii) the characteristic velocity of the x_B field $V_D = \sqrt{D_\mathrm{B}/\tau_D}$, $D_\mathrm{B} = M_x \partial \mu_\mathrm{B}/\partial x_\mathrm{B}$. Here, D_η, D_φ and D_B are the diffusion coefficients for propagation of the η, φ and x_B fields, respectively.

The speeds V_η, V_φ and V_D characterize the relaxation to local equilibrium with the characteristic times τ_η, τ_φ and τ_D (see the general theory in the monograph [39]). The influence of these parameters on the growth kinetics has, for instance, been shown in the phase-field analysis of solute trapping [40] in comparison with experiments in which the local non-equilibrium contribution to solute diffusion led to diffusionless solidification. The role of the local non-equilibrium contribution to crystal growth at high undercoolings, where disorder trapping occurs together with the kinetic transition, will be analysed in forthcoming works.

8. Summary

Consistent with previous experimental observations, we found that a steep increase in the interface velocity occurs at a critical undercooling, connected with a sharp decrease in the order parameter.

— By analysing the complete scenario of disorder trapping from low to high crystal growth velocities, the conditions for disorder trapping during competition of two diffuse interfaces were formulated.
— A phase-field model which includes both a diffuse crystal/liquid interface and a diffuse ordering zone has been put forward. The model consists of governing equations for mass transport by atomic diffusion, dynamics of the phase field and dynamics of atomic ordering.
— Results of phase-field modelling show that complete disorder trapping can be consistently described as a kinetic phase transition [16] in the atomic structure of a growing crystal.
— Disorder trapping shares both similarities and differences with solute trapping, as both describe a kinetic phase transition in non-equilibrium solidification.

Data accessibility. This article has no additional data.
Authors' contributions. All the authors contributed equally to the present research paper.
Competing interests. The authors declare that they have no competing interests.
Funding. This work was supported by the Russian Science Foundation (grant no. 16-11-10095), the German Space Center Space Management (under contract number 50WM1541) and the Deutsche Forschungsgemeinschaft (DFG) (under grant no. Re1261/8-2).

References

1. Chernov AA. 1984 *Modern crystallography III. Crystal growth*. Berlin, Germany: Springer.
2. Barth M, Wei B, Herlach DM. 1995 Crystal growth in undercooled melts of the intermetallic compounds FeSi and CoSi. *Phys. Rev. B* **51**, 3422–3428. (doi:10.1103/PhysRevB.51.3422)
3. Hartmann H, Holland-Moritz D, Galenko PK, Herlach DM. 2009 Evidence of the transition from ordered to disordered growth during rapid solidification of an intermetallic phase. *Europhys. Lett.* **87**, 40007. (doi:10.1209/0295-5075/87/40007)
4. Ahmad R, Cochrane RF, Mullis AM. 2012 Disorder trapping during the solidification of βNi_3Ge from its deeply undercooled melt. *J. Mater. Sci.* **47**, 2411–2020. (doi:10.1007/s10853-011-6062-y)
5. Yang C, Gao J. 2014 Dendritic growth kinetics and disorder trapping of the intermetallic compound Ni_3Sn under a static magnetic field. *J. Cryst. Growth* **394**, 24–27. (doi:10.1016/j.jcrysgro.2014.02.015)
6. Boettinger WJ, Aziz MJ. 1989 Theory for the trapping of disorder and solute in intermetallic phases by rapid solidification. *Acta Metall.* **37**, 3379–3391. (doi:10.1016/0001-6160(89)90210-1)
7. Greer AL, Assadi H. 1997 Rapid solidification of intermetallic compounds. *Mater. Sci. Eng. A* **226–228**, 133–141. (doi:10.1016/S0921-5093(97)80032-9)
8. Assadi H. 2007 A phase-field model for non-equilibrium solidification of intermetallics. *Acta Mater.* **55**, 5225–5253. (doi:10.1016/j.actamat.2007.05.042)
9. Zhang XQ, Yang Y, Gao YF, Hoyt JJ, Asta M, Sun DJ. 2012 Disorder trapping during crystallization of the B2-ordered NiAl compound. *Phys. Rev. B* **85**, 041601-1–7. (doi:10.1103/PhysRevE.85.041601)
10. Alster E, Elder KR, Hoyt JJ, Voorhees PW. 2017 Phase-field-crystal model for ordered crystals. *Phys. Rev. E* **95**, 022105. (doi:10.1103/PhysRevE.95.022105)
11. Voronkov VV, Falster R. 2002 Intrinsic point defects and impurities in silicon crystal growth. *J. Electrochem. Soc.* **149**, G167–G174. (doi:10.1149/1.1435361)
12. Voronkov VV, Chernov AA. 1967 Solute trapping during motion of the elementary step. *Kristallografiya* **12**, 222–229.
13. Aziz M, Kaplan T. 1988 Continuous growth model for interface motion during alloy solidification. *Acta Metall.* **36**, 2335–2347. (doi:10.1016/0001-6160(88)90333-1)
14. Eckler K, Cochrane RF, Herlach DM, Feuerbacher B, Jurisch M. 1992 Evidence for a transition from diffusion-controlled to thermally controlled solidification in metallic alloys. *Phys. Rev. B* **45**, 5019–5022. (doi:10.1103/PhysRevB.45.5019)
15. Galenko P. 2007 Solute trapping and diffusionless solidification in a binary system. *Phys. Rev. E* **76**, 031606. (doi:10.1103/PhysRevE.76.031606)
16. Chernov AA. 1968 Kinetic phase transitions. *Sov. Phys. JETP* **26**, 1182–1190.
17. Chernov AA. 1970 Growth of copolymer chains and mixed crystals—trial and error statistics. *Sov. Fis. Usp.* **13**, 101–128. (doi:10.1070/PU1970v013n01ABEH004200)
18. Temkin DE. 1971 Kinetic phase transition during a phase conversion in a binary alloy. *Sov. Phys. Cryst.* **15**, 773–780.
19. Brener EA, Temkin DE. 1983 Kinetics of normal growth of ordering crystal. *Sov. Phys. Cryst.* **28**, 7–16.
20. Brener EA, Temkin DE. 1983 Kinetic transition during the growth of a crystal under ordering. *Sov. Phys. Cryst.* **28**, 142–149.
21. Boettinger WJ, Warren JA, Beckermann C, Karma A. 2002 Phase-field simulation of solidification. *Annu. Rev. Mater. Res.* **32**, 163–194. (doi:10.1146/annurev.matsci.32.101901.155803)
22. Emmerich H, Löwen H, Wittkowski R, Gruhn T, Tóth GI, Tegze G, Gránásy L. 2012 Phase-field-crystal models for condensed matter dynamics on atomic length and diffusive time scales: an overview. *Adv. Phys.* **61**, 665–743. (doi:10.1080/00018732.2012.737555)
23. Steinbach I. 2013 Phase-field model for microstructure evolution at the mesoscopic scale. *Annu. Rev. Mater. Res.* **43**, 89–107. (doi:10.1146/annurev-matsci-071312-121703)
24. Galenko P, Jou D. 2005 Diffuse-interface model for rapid phase transformations in nonequilibrium systems. *Phys. Rev. E* **71**, 046125. (doi:10.1103/PhysRevE.71.046125)

25. Lebedev VG, Sysoeva AV, Galenko PK. 2011 Unconditionally gradient-stable computational schemes in problems of fast phase transitions. *Phys. Rev. E* **83**, 026705. (doi:10.1103/PhysRevE.83.026705)
26. Mandel'shtam LI, Leontovich MA. 1937 On the theory of adsorption of sound in liquids. *Zh. Eksp. Teor. Fiz.* **7**, 438–449.
27. Patashinskii AZ, Pokrovskii VL 1979 *Fluctuation theory of phase transitions*. Oxford, UK: Pergamon Press.
28. Lifshitz EM, Pitaevskii LP 1981 *Physical kinetics. Course of theoretical physics*. Oxford, UK: Pergamon Press.
29. Allen SM, Cahn JW. 1979 A microscopic theory for antiphase boundary motion and its application to antiphase domain coarsening. *Acta Metall.* **27**, 1085–1095. (doi:10.1016/0001-6160(79)90196-2)
30. Vasin MG, Ladianov VI. 2003 Structural transitions and nonmonotonic relaxation processes in liquid metals. *Phys. Rev. E* **68**, 051202. (doi:10.1103/PhysRevE.68.051202)
31. Galenko P, Lebedev V. 2008 Non-equilibrium effects in spinodal decomposition of a binary system. *Phys. Lett. A* **372**, 985–989. (doi:10.1016/j.physleta.2007.08.070)
32. Galenko P, Danilov D, Lebedev V. 2009 Phase-field-crystal and Swift-Hohenberg equations with fast dynamics. *Phys. Rev. E* **79**, 051110. (doi:10.1103/PhysRevE.79.051110)
33. Galenko PK, Herlach DM. 2006 Diffusionless crystal growth in rapidly solidifying eutectic systems. *Phys. Rev. Lett.* **96**, 150602. (doi:10.1103/PhysRevLett.96.150602)
34. Yang Y, Humadi H, Buta D, Laird BB, Sun D, Hoyt JJ, Asta M. 2011 Atomistic simulations of nonequilibrium crystal-growth kinetics from alloy melts. *Phys. Rev. Lett.* **107**, 025505. (doi:10.1103/PhysRevLett.107.025505)
35. Jou D, Galenko P. 2013 Coarse graining for the phase-field model of fast phase transitions. *Phys. Rev. E* **88**, 042151. (doi:10.1103/PhysRevE.88.042151)
36. Herlach DM, Galenko PK, Holland-Moritz D. 2007 *Metastable solids from undercooled melts*. Amsterdam, The Netherlands: Elsevier.
37. Hartmann H, Galenko PK, Holland-Moritz D, Kolbe M, Herlach DM, Shuleshova O. 2008 Nonequilibrium solidification in undercooled $Ti_{45}Al_{55}$ melts. *J. Appl. Phys.* **103**, 073509. (doi:10.1063/1.2903920)
38. Galenko PK, Danilov DA. 1997 Local nonequilibrium effect on rapid dendritic growth in binary alloy melt. *Phys. Lett. A* **235**, 271–280. (doi:10.1016/S0375-9601(97)00562-8)
39. Jou D, Casas-Vazquez J, Lebon G 2010 *Extended irreversible thermodynamics*, 4th edn. Berlin, Germany: Springer.
40. Galenko PK, Abramova EV, Jou D, Danilov DA, Lebedev VG, Herlach DM. 2011 Solute trapping in rapid solidification of a binary dilute system: a phase-field study. *Phys. Rev. E* **84**, 041143. (doi:10.1103/PhysRevE.84.041143)